Correspondence

Internal Dielectric Transduction: Optimal Position and Frequency Scaling

Dana Weinstein and Sunil A. Bhave

***Abstract*—We propose the optimal design for "internal dielectric transduction" of longitudinal bulk mode resonators. This transduction increases in efficiency as the dielectric thickness approaches half the acoustic wavelength. With dielectric films at positions of maximum strain (minimum displacement) in the resonator, 60 GHz resonators are proposed with 50 Ω motional impedance.**

I. Introduction

With quality factors (Q) often exceeding 10,000, vibrating micromechanical resonators have emerged as leading candidates for on-chip versions of high-Q resonators used in wireless communications systems. However, extending the frequency of micro electromechanical systems (MEMS) resonators generally entails scaling of resonator dimensions leading to increased motional impedance.

Most electrostatic MEMS resonators to date use air-gap capacitive transduction to drive and sense resonant motion. Dielectric electrostatic transduction has several benefits over common air-gap transduction: it is desirable in order to achieve smaller capacitive gaps, to prevent pull-in and stiction symptomatic of air-gap transducers, and to enhance driving force and capacitive sensing due to high dielectric permittivity. Therefore, dielectrics can extend resonant frequencies to the >5 GHz range at which these issues are most prominent. However, most devices demonstrated to date are geometrically identical to their air-gap counterparts, with a dielectric film in place of the air-gap transducer. As resonators scale to higher frequencies and smaller dimensions, this transduction configuration may not be the most suitable.

Recently, Kaajakari *et al.* [1] calculated the relative performance of various electrode configurations for transduction of electrostatic resonators. Comparing air gap, in-plane (lateral or Poisson) dielectric [2], and internal (vertical) dielectric transduction, they concluded that internal transduction performs poorly relative to the other two modes of transduction. This paper more closely investigates dielectric thickness and position optimization of the dielectric films in internal transduction, showing promising performance scaling to ultra-high frequencies.

Manuscript received May 9, 2007; accepted August 6, 2007.

The authors are with Cornell University, Ithaca, New York (e-mail: dw222@cornell.edu).

Digital Object Identifier 10.1109/TUFFC.2007.598

Before continuing with the analysis of this transduction method, it is necessary to address the difference between internal and external dielectric transduction. Both mechanisms use dielectric drive and sense transducers. However, external transduction [3], [4] assumes free boundary conditions (zero stress) at the dielectric interface, driving at a frequency corresponding to a resonant mode with maximum displacement at the dielectric, and necessitating maximum acoustic mismatch between the dielectric and resonator bulk. However, internal transduction assumes a close acoustic match between the bulk resonator and dielectric film, integrating the dielectric into the resonant mode shape, as discussed in the following sections.

II. Equation of Motion

A longitudinal-mode bar resonator is driven and sensed electrostatically with thin vertical dielectric layers, as shown in Fig. 1. The resonator body is biased to V_{DC}, and a harmonic excitation of amplitude v_{in} is applied to the drive electrode at resonant frequency. Internal transduction requires that the dielectric films be acoustically matched to the bulk resonator material, thereby maintaining the mode shape and frequency of the resonator without degrading the quality factor. With this assumption, the n^{th} harmonic of the free-free longitudinal mode bar spanning $-L/2 \le x \le L/2$ has displacement following:

$$u(x,t) = U_0 e^{i2\pi \cdot f_n t} \sin(k_n x), \quad n \text{ odd}, \tag{1}$$

where $k_n = n\pi/L$ and U_0 is the maximum amplitude of vibrations of the bar. Fig. 2 illustrates the third harmonic of this longitudinal mode. The resonant frequency of the n^{th} harmonic is $f_n = (n/2L)\sqrt{Y/\rho}$ for Y and ρ the Young's modulus and mass density of the bar, respectively. The driving dielectric film of thickness g is placed at $x = d$ in the resonator (Fig. 1). The alternating current (AC) component of the capacitive force across the dielectric of permittivity ε_f is:

$$f(x,t) = \frac{\varepsilon_f A}{g^2} V_{DC} v_{\text{in}} e^{i2\pi \cdot f_n t} \; \forall x \in \left[d - \frac{g}{2},\; d + \frac{g}{2} \right]. \tag{2}$$

Given the equation of motion for damped vibrations in a bar [5]:

$$\rho A \frac{\partial^2 u(x,t)}{\partial t^2} - bA \frac{\partial^3 u(x,t)}{\partial t \partial x^2} - YA \frac{\partial^2 u(x,t)}{\partial x^2} = \frac{\partial f(x,t)}{\partial x}, \tag{3}$$

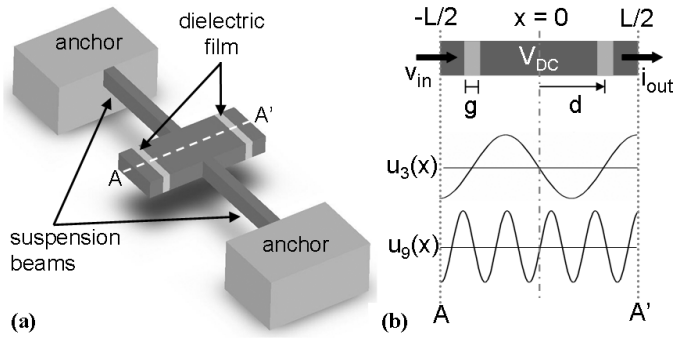

Fig. 1. (a) Schematic of dielectrically transduced free-free longitudinal bulk mode resonator. The dielectric films are incorporated into the resonator, driving and sensing electrostatically. (b) Cross section of bar resonator. A bias voltage V_{DC} is applied to the resonator. An AC voltage $v_{\rm in}$ on one end drives resonance, and an output current $i_{\rm out}$ is measured at the other. The normalized amplitudes of the third and ninth longitudinal mode harmonics are displayed.

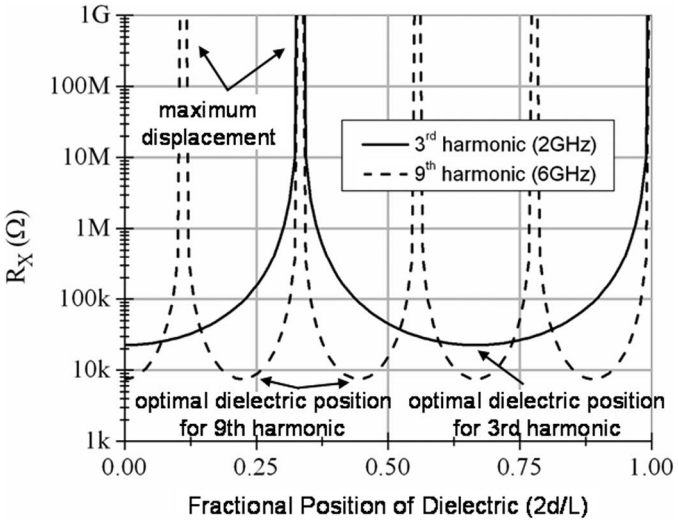

Fig. 2. R_X as a function of fractional dielectric position $|d/(L/2)|$ for the third and ninth harmonic longitudinal (width-extensional) modes of a 6.4-μm long bar. $g = 10$ nm, resonator thickness is 2.5 μm, width is 40 μm, $V_{DC} = 10$ V, $\varepsilon_f = 7\varepsilon_0$ and Q is 5000.

and substituting (1) into (3), the amplitude of vibrations at resonant frequency is given by:

$$U_0 = \frac{2Q\varepsilon_f V_{DC} v_{\rm in}}{n^2\pi^2 Y}\frac{L}{g^2} \cdot \left[\sin\left(k_n d - \frac{k_n g}{2}\right) - \sin\left(k_n d + \frac{k_n g}{2}\right)\right], \quad (4)$$

for Q the quality factor of the resonator. This resonance is detected by the changing capacitance due to vibrations at the sensing dielectric film:

$$\begin{aligned} i_{\rm out} &= V_{DC}\frac{dC}{dt} = V_{DC}\frac{dC}{du}\frac{du}{dt} \\ &= \frac{\varepsilon_f V_{DC} A}{g^2}\left[\sin\left(k_n d - \frac{k_n g}{2}\right) - \sin\left(k_n d + \frac{k_n g}{2}\right)\right] \\ &\quad \cdot 2\pi \cdot f_n U_0 \quad (5) \\ &= \frac{2Q\varepsilon_f^2 V_{DC}^2 A}{n\pi\sqrt{Y\rho}g^4}\left[\sin\left(k_n d - \frac{k_n g}{2}\right) - \sin\left(k_n d + \frac{k_n g}{2}\right)\right]^2 \\ &\quad \cdot v_{\rm in}, \end{aligned}$$

resulting in a motional impedance:

$$\begin{aligned} R_X &\equiv \frac{v_{\rm in}}{i_{\rm out}} \\ &= \frac{n\pi\sqrt{Y\rho}}{2QA\varepsilon_f^2 V_{DC}^2}\frac{g^4}{[\sin(k_n d - k_n g/2) - \sin(k_n d + k_n g/2)]^2}, \end{aligned} \quad (6)$$

simplifying to:

$$R_X = \frac{n\pi\sqrt{Y\rho}}{2QA\varepsilon_f^2 V_{DC}^2}\frac{g^4}{\cos^2(k_n d)\sin^2(k_n g/2)}. \quad (7)$$

III. Optimization

Eq. (7) provides a great deal of insight into designing an optimal bulk-mode resonator using internal dielectric transduction. As expected, the quartic dependence of the motional impedance on dielectric thickness necessitates the thinnest dielectric possible. This is generally defined by limitations in fabrication and material properties. Furthermore, this form for the motional impedance, differing from air-gap transduction primarily by the trigonometric terms in the denominator, indicates that the position of both drive and sense dielectric films should be centered at a displacement minimum, or strain maximum. This choice for the position of the dielectric films sets $\cos^2(k_n d) = 1$, minimizing R_X with respect to d.

The $\sin^2$ term in the denominator of (7) results from the modal displacement at the dielectric-bulk resonator interface. As noted in [1], this factor degrades the performance of the resonator considerably at low frequencies at which the acoustic wavelength $\lambda \gg g$. However, as the resonator scales to higher frequencies, and $\lambda/2 \to g$, the $\sin^2$ term in the denominator approaches unity, reducing motional impedance. Consequently, for a fixed dielectric thickness g determined by fabrication limitations, there is an optimal frequency of operation with acoustic wavelength $\lambda = 2 \cdot g$.

Fig. 2 presents the R_X of the third and ninth harmonics of an internally transduced longitudinal bar, varying the dielectric position along the length of the resonator. A constant Q of 5000 is used for both the third and ninth harmonics. Although in an ideal, isolated resonator made of a defect-free, single-crystal material, the quality factor scales as $Q \propto 1/f$, silicon resonators have not yet reached this scaling limit, demonstrating increased $f \cdot Q$ in recent years [6]. Because the Q of these silicon resonators exhibits a strong dependence on many design parameters, it is considered constant for simplicity.

As shown in Fig. 2, minima in the motional impedance occur for points of maximum strain (minimum displacement). The large spatial range near the displacement minima over which R_X is low allows for fabrication of reliable

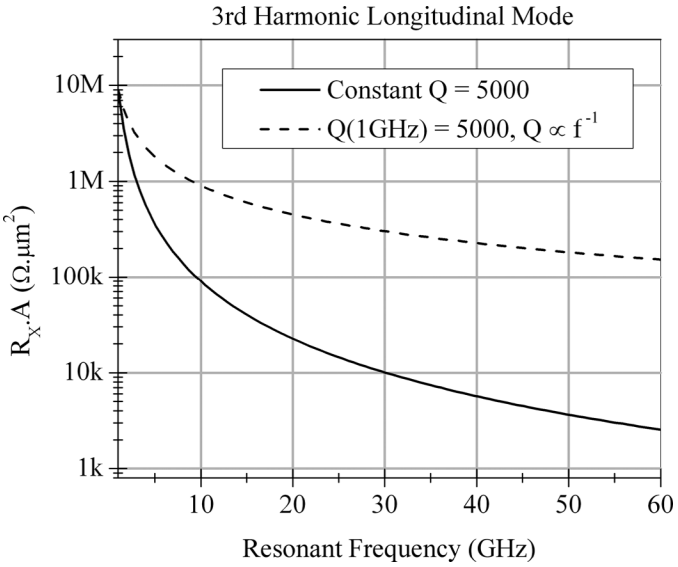

Fig. 3. R_X scaling with frequency, normalized to the cross-sectional area of the resonator. $g = 10$ nm, $V_{DC} = 10$ V, and $\varepsilon_f = 7\varepsilon_0$. The dielectric films are placed at maximum strain. Frequency scaling trends for a constant Q of 5000 (solid line) and $Q \propto 1/f$ (dashed line) are shown.

devices despite misalignment tolerances. The coincidence of displacement minima of the third and ninth harmonics at the fractional dielectric position of 2/3 allows for the optimal excitation of both modes in the same device. This may be useful for multifrequency applications. However, if multiple modes are undesired, the third harmonic can be suppressed by placing the dielectric at a fractional dielectric position of 2/9 or 4/9, near a displacement maximum of the third harmonic, while still driving the ninth harmonic at maximum strain.

Frequency scaling of the bulk mode longitudinal resonators using internal dielectric transduction is shown in Fig. 3. The motional impedance, normalized to the cross-sectional area of the resonator, decreases drastically with increasing frequency, achieving $k\Omega \cdot \mu m^2$ impedances at 60 GHz. Again, a constant Q of 5000 is assumed (solid line in Fig. 3) for simplicity due to the strong dependence of Q on design parameters. The dashed line in Fig. 3 presents frequency scaling of transduction for $Q \propto 1/f$, with a Q of 5000 at 1 GHz. The frequency scaling result of Fig. 3 converges to an film bulk acoustic resonator (FBAR)-like resonator or the Bragg reflector for a solid-mounted bulk acoustic wave (BAW) resonator, stacking multiple dielectrics of thickness $\lambda/2$ between conductive layers of the same thickness. Recently, such devices have been demonstrated successfully in the 10 GHz range [7].

Common dielectrics such as silicon dioxide ($\kappa \sim 3.9$) and silicon nitride ($\kappa \sim 7$) perform reliably in films as thin as a few nanometers. For such transduction film thickness, the motional impedance is minimized at >50 GHz, but that may be too high for 1–10 GHz operation. Low impedance resonators in the radio and microwave frequency range can be achieved by using high-k dielectric materials, such as barium strontium titanate (BST). Although BST films are not electrically reliable below ~200 nm, they exhibit a high permittivity often exceeding 300. This will prove to be a great advantage in obtaining low-impedance internally transduced resonators at low-gigahertz frequencies. Minimizing (7) with respect to resonant frequency for a 200 nm dielectric film, one obtains an optimal frequency of operation at 10.7 GHz. Assuming a Q of 5000 and a bias voltage of 20 V, this structure has $10\ k\Omega \cdot \mu m^2$ impedance at a third harmonic resonance. For instance, a 50 Ω BST resonator at 10 GHz can be obtained by stacking the bulk/dielectric layers vertically (thickness extensional mode) with a 10-μm × 20-μm footprint, or by forming a 2-μm thick extensional ring [8] with an approximate radius of 16 μm.

IV. Conclusions

Although the motional impedance in (4) differs from air-gap R_X primarily by the sin terms in the denominator, the dielectric thickness g can be fabricated much smaller than air gaps, and the permittivity ε_f enhances resonator performance. We offer a dielectric transduction configuration, optimizing dielectric film position centered at strain maxima. The dielectric films can be stacked periodically in the displacement nodes of higher-harmonic bulk resonator, further improving R_X. Although internal dielectric transduction performs poorly at low frequencies at which the acoustic wavelength is much longer than the dielectric thickness, it is an attractive solution for electrostatic resonators at ultra-high frequencies.

References

[1] V. Kaajakari, A. T. Alastalo, and T. Mattila, "Electrostatic transducers for micromechanical resonators: Free space and solid dielectric," *IEEE Trans. Ultrason., Ferroelect., Freq. Contr.*, vol. 53, no. 12, pp. 2484–2489, 2006.

[2] S. A. Bhave and R. T. Howe, "Silicon nitride-on-silicon bar resonator using internal electrostatic transduction," in *Proc. 13th Int. Conf. Solid-State Sens., Actuators Microsyst.*, June 5–9, 2005, pp. 2139–2142.

[3] S. A. Bhave and R. T. Howe, "Internal electrostatic transduction for bulk-mode MEMS resonators," in *Proc. Solid State Sens., Actuator Microsyst. Workshop*, June 6–10, 2004, pp. 59–60.

[4] Y.-W. Lin, S.-S. Li, Y. Xie, Z. Ren, and C. T.-C. Nguyen, "Vibrating micromechanical resonators with solid dielectric capacitive transducer gaps," in *Proc. IEEE Freq. Contr. Symp.*, 2005, pp. 128–134.

[5] B. A. Auld, *Acoustic Fields and Waves in Solids*. 2nd ed. Malabar, FL: Kreiger, 1990.

[6] C. T.-C. Nguyen, "MEMS technology for timing and frequency control," *IEEE Trans. Ultrason., Ferroelect., Freq. Contr.*, vol. 54, no. 2, pp. 251–270, 2007.

[7] S. Gevorgian, A. Vorobiev, and T. Lewin, "DC field and temperature dependent acoustic resonances in parallel-plate capacitors based on $SrTiO_3$ and $Ba_{0.25}Sr_{0.75}TiO_3$ films: Experiment and modeling," *J. Appl. Phys.*, vol. 99, art. no. 124112, 2006.

[8] B. Bircumshaw, G. Liu, H. Takeuchi, T.-J. King, R. T. Howe, O. O'Reilly, and A. Pisano, "The radial bulk annular resonator: Towards a 50 Ω RF MEMS filter," in *Proc. IEEE 12th Int. Conf. Solid State Sens., Actuators Microsyst.*, June 8–12, 2003, pp. 875–878.